

A Study of Reduced Graphene Oxide – Cu Nanocomposite for the High Performance Electrochemical Supercapacitor Application

Shikha Upadhyay^{1*}, Dr. Harbeer Singh²

¹ Research Scholar, The Glocal University

² Research Supervisor, The Glocal University

Abstract - The modern electrochemical energy storage device, the supercapacitor, has several advantageous properties, including high power density, quick charge rates, long-life cycle stability, high specific capacitance, and low cost. Nanostructured materials, such as metals, metal oxides, and graphene nanosheets, have been increasingly employed in recent years for energy storage. In this study, nanocomposites of metal/metal-oxide decorated reduced graphene oxide (M/MO-rGO) were fabricated through a simple, low-cost chemical reduction process employing hydrazine hydrate as the reducing agent and metal precursors and graphene oxide powder as the starting materials. The three synthesized rGO-based nanocomposite reported in this study are bismuth oxide decorated rGO (Bi₂O₃@rGO) nanocomposite containing different Bi(NO₃)₃ concentrations varying from 5mM to 25mM, (ii) silver decorated rGO (Ag@rGO) nanocomposite containing 0.5 g AgNO₃ and (iii) iron oxide decorated rGO (Fe₃O₄/rGO) nanocomposite with different Fe(NO₃)₃ content varying from 5mM to 25mM.

Keywords - Reduced graphene oxide, nanocomposite, high performance, electrochemical, super capacitor, application.

-----X-----

INTRODUCTION

The term "nanotechnology" is often used to refer to the study, creation, and use of nanoscale components and systems. Nanotechnology also includes research into the underlying physics of nanomaterials and nanostructures. Studying the fundamental connections between macroscopic physical properties and events and tiny material dimensions is what nanoscience is all about. In the United States, nanotechnology is defined as the study and use of materials and systems whose structures and components exhibit novel and significantly increased physical, chemical, and biological features, phenomena, and processes due to their nanoscale size (Cao, 2011). Exploring new physical features and phenomena and realizing future applications of nanostructures and nanomaterials hinge on the ability to manufacture and process nanoparticles and nanostructures. Materials having at least one dimension in the nanometer range are included in the category of nanostructured materials. This includes thin films, nanorods and nanowires, nanoparticles, and bulk materials (Fernández, 2018).

Capacitors

To store electrostatic energy, you may use a capacitor, which is a passive device with two electric terminals and no moving parts. Capacitors come in a wide

variety of shapes and sizes, but they always have the same basic structure: two electric conductor plates separated by a dielectric. Capacitors come in a wide variety of shapes and sizes, but they always have the same basic structure: two electric conductor plates separated by a dielectric. Capacitors may be made from a wide range of materials, including metal thin sheets, aluminum foil, and disks. Capacitors' ability to store electrical energy is improved by a dielectric, which is itself nonconductive. While capacitors have been around for 200 years, the technology behind modern capacitors has only been around for 50 years. During the last fifty years, several technologies have been invented for the creation of improved capacitors. In contrast to their power, capacitors' limited energy storage capacity limits their usefulness. Electrostatic capacitors, which are the most common kind of capacitor, include two conducting electrodes separated by an insulator called a dielectric (Schueth, 2014).

Supercapacitors

Conversion equipment, such as supercapacitors, is a new kind of energy-saving technology with the desirable properties of high power density, rapid discharge charge, good circulation aspect, absence of self-discharging, safe operation, and cheap cost.

Because of their extensive electrochemical properties, supercapacitors are often constructed using porous materials like MOs, carbon-based composites of M/MOs, and other composites like graphene-based M/MOs. regular form factor for a supercapacitor. Similar to the sandwiched architecture of capacitors, supercapacitors consist of two very porous electrodes. These two electrodes are immersed in an electrolyte and separated by a dielectric membrane through which ions may flow (Karthik, 2014). When subjected to an external electric field, the device's two electrodes attract and collect opposite charges, or positive and negative ions, respectively. Electrolyte ions diffuse through the separator and into the electrode pores in accordance with the natural attraction rule of opposing charges. Ion recombination is prevented by the electrodes' design as well. The outcome is a double layer of charges at each electrode.

Principle of supercapacitor

A supercapacitor is based on the same basic idea as a regular capacitor. Supercapacitors, like regular capacitors, have two electrodes separated by an insulating dielectric. The large surface areas of electrode material in supercapacitors, in comparison to normal capacitors, and an electrolyte solution are the primary differentiating factors between the two kinds of devices. When the surface area of a supercapacitor expands and the distance between its electrodes decreases, the device's capacitance and energy density skyrocket (Lakra, 2021).

Graphene, Graphene oxide (GO)

Graphene, an allotrope of elemental carbon, was found to be the first 2D crystal, with its sp^2 -bonded honeycomb arrangement. Sir Andre Konstantin Geim, a physicist, and Sir Konstantin Sergeevich Novoselov, also a physicist, worked together to devise a simple but successful technique for exfoliating a single layer of HOPG highly orientated pyrolytic graphite using common scotch tape. Since its discovery, this allotrope has quickly surpassed CNTs and activated carbons as the preferred electrode material for supercapacitors and captivated an entire scientific and technological province due to its extraordinary properties such as high specific surface area, anomalous quantum Hall effect, high thermal conductivity, outstanding mechanical strength, high optical transmittance, high young modulus, etc (Park, 2010).

In 2010, the Nobel Prize in Physics was awarded for the discovery of this extraordinary substance. This has led some to argue that graphene is the precursor of all graphitic materials, including buckyballs, CNTs, and graphite. The energy conversion and storage applications of graphene-based materials are among the most recognized and researched. These applications span a wide range of fields, including supercapacitors, batteries, LEDs, biomedicine, sensors, photovoltaics, and many more. In general, a single sheet of graphene may achieve long-term stability, high power, and high energy densities, as

well as specific capacitances of up to 21 mFcm⁻² and 550 F/g (Phan, 2018).

Graphene

Graphene has been dubbed a "wonder material" because to its exceptional physical and chemical features, and it has several applications across many fields. Graphene's strong conductivity, for instance, makes it a desirable material in electronics, where it also demonstrates chemical resistance, exceptional optical clarity, and mechanical stability. Being a single-layer, foldable material with a theoretical surface area of 2630 m² g⁻¹, it is an excellent alternative to indium tin oxide (ITO) for use in solar cell fabrication and energy storage devices (Rashidi, 2020).

As compared to graphite (10 m² g⁻¹) and SWCNTs (1315 m² g⁻¹) as electrode materials, graphene stands out and garners a lot of interest. Graphene has been extensively reported as an electrode material in supercapacitor technologies, lithium-ion batteries, and fuel cells. When a large quantity of the material is needed, chemical methods are favored for the synstudy of bulk chemically reduced graphene oxide (rGO) over the production of individual graphene layers (Yan, 2018). Just its use in supercapacitors will be discussed in this study. The capacity to insert oxygenated groups on both the basal and edge planes through covalent and non-covalent functionalization is perhaps the most important trait of graphene after considering its physical and chemical qualities (Zhao, 2020).

RESEARCH METHODOLOGY

Synstudy protocols for rGO-based samples are provided, as is a review of the various experimental methods utilized to describe them. Methods such as scanning electron microscopy (SEM), X-ray diffraction (XRD), Fourier transform infrared spectroscopy (FTIR), and ultraviolet-visible spectroscopy (UV-Vis) are all a part of this category of testing. In addition, the experimental methods utilized for electrochemical and electrical measurement were briefly discussed.

Experimental Procedure

Materials: Graphite fine powder (98%), potassium permanganate (KMnO₄), sulfuric acid (H₂SO₄, 98%), sodium nitrate (NaNO₃), hydrochloric acid (HCl), hydrogen peroxide (H₂O₂, 30 wt.%), hydrazine hydrate (H₂N-NH₂), Ethanol (C₂H₅-OH), Bismuth (III) Nitrate Pentahydrate (Bi(NO₃)₃·5H₂O) powder, silver nitrate (AgNO₃) and Ferric Nitrate (Fe(NO₃)₂·9H₂O) are procured from Sigma-Aldrich. The DI water has been used for cleaning and disinfecting. The experiment only used high-quality, analytical-grade substances.

Synstudy of Graphene-Oxide (GO): Synstudy of graphene oxide (GO) was achieved by adapting Hummer's method. This synstudy called for 5 grams

of graphite powder to be combined with 110 milliliters of 98% concentrated H₂SO₄ and 2.5 grams of NaNO₃. For thirty minutes, the aforementioned mixture was mixed at room temperature. A dark slurry developed once the ingredients were thoroughly blended. After that, the beaker containing the reaction mixture was put into an ice bath to bring the temperature down to below 20 degrees Celsius. As the temperature dropped far below 20 °C, 15 g of KMnO₄ powder was cautiously added, pinch by pinch, while swirling vigorously to prevent explosion and overheating.

The production of manganese heptoxide causes the solution to take on a greenish hue at this point. After then, the heat was turned up to 35 degrees Celsius, and stirring went on for another two hours. Graphite oxidation causes the mixture to thicken and change color to a dark brownish orange throughout this period. Next, 300 ml of DI was slowly added to dilute it. The mixture was heated to 98 degrees Celsius while being agitated for an additional hour. Once the solution had cooled for a few hours at room temperature, 15 ml of H₂O₂ (30%) was added to halt the reaction. To remove metal ions from the resulting compounds, they are filtered and washed many times with a 10% HCl solution, DI water, and ethanol. After 12 hours of air drying at room temperature, the GO has been thoroughly cleaned and filtered.

- Reduced Graphene Oxide (rGO) Production
- Synstudy of Bismuth-oxide/rGO (Bi₂O₃@rGO) Nanocomposite
- Synstudy of Silver/rGO (Ag@rGO) Nanocomposite
- Synstudy of iron-oxide decorated reduced graphene oxide (Fe₃O₄/rGO) nanocomposites via simple chemical reduction method

Morphological, Structural, Chemical and Optical Characterization Techniques

- Scanning Electron Microscope (SEM) and Electron Dispersive Xray (EDX)
- Transmission electron microscopy (TEM)
- X-ray diffraction (XRD)
- Fourier transform infrared spectroscopy (FTIR)
- Raman Spectroscopy
- X-ray photoelectron spectroscopy (XPS)
- UV-Visible Spectroscopy

Electrical Measurement

Current–voltage (I–V) characteristic curves show how a material responds to varying voltage across its terminals. I-V measurements of GO, rGO, Bi₂O₃@rGO, Ag@rGO, and Fe₃O₄/rGO nanocomposites were performed using a KEYSIGHTB2901A precession source/measure unit. To prepare samples for the IV measurement, a paste was made by combining the samples with a small quantity of ethanol, and then a very thin layer (0.1 mg)

of the paste was applied to the ITO substrate using a brush.

RESULTS

Morphology of Bi₂O₃@rGO Nanocomposites

Here are some SEM pictures of reduced graphene oxide that has been coated with bismuth oxide. The SEM pictures of 5mM and 10mM Bi₂O₃@rGO nanocomposite revealed the cauliflower-like morphology of rGO coated with Bi₂O₃ nanoparticles. By contrast, scanning electron micrographs of Bi₂O₃@rGO nanocomposites with a Bi(NO₃)₃ concentration between 15 mM and 25 mM reveal an abundance of exquisite nanoscale flowers dispersed throughout the rGO corrugations. The chemicals have a propensity to form aggregates, taking the shape of irregular particles or fluffy nanoflowers. The morphological shift from 5mM to 25mM Bi₂O₃@rGO nanocomposite is indicative of the creation of Bi₂O₃ nanoparticles in rGO sheets, and an increase in Bi₂O₃ nanoparticle number was seen when Bi(NO₃)₃ concentration increased from 5mM to 25mM. Therefore, increasing the amount of Bi(NO₃)₃ in the nanocomposite causes a change in its structure.

Nanoscale flower-shaped structures and irregular particles ranged in size from 1.378 to 9.563 micrometers in diameter and length, respectively. The Bi₂O₃ nanoparticles were measured to have an average size between 103 nm and 326 nm, indicating that they were successfully produced. Thus, rGO is a great material for supercapacitors and photocatalysis because of its adaptability and conductivity. Nanoparticles of Bi₂O₃ are liberally sprinkled over the rGO sheets, indicating strong intra-sheet interactions. A strong ionic bond was established between the GO sheets and the Bi³⁺ precursors during Bi₂O₃@rGO nanocomposite formation, allowing for the easy uptake of Bi³⁺ cations by the GO sheets at diverse reaction sites. Hence, following the chemical reduction activity, Bi₂O₃ nanoparticles were spread evenly and attached strongly to rGO sheets.

This led to the formation of Bi₂O₃ nanoparticles from Bi³⁺ precursors and the reduction of GO into rGO. The SEM results for the Bi₂O₃@rGO nanocomposite therefore corroborate the interaction of Bi₂O₃ with the rGO sheets.

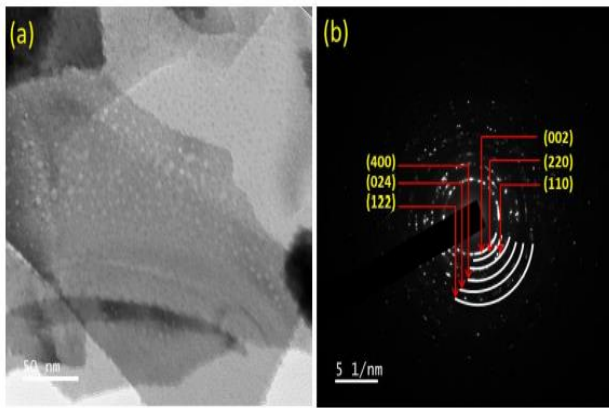


Figure 1: (a) FETEM image and (b) selected area electron diffraction (SAED) pattern of Bi₂O₃@rGO nanocomposite

Structural characterization of Bi₂O₃@rGO nanocomposites

The XRD spectra of graphite reveal a high peak at $2\theta = 26.60^\circ$ and a faint peak at 54.72° , which correspond to (002) and (004) planes with d-spacing of 3.34 and 1.67, respectively, and were compared to those of Bi₂O₃@rGO nanocomposites with varying concentrations of Bi(NO₃)₃. The X-ray diffraction (XRD) spectra of Bi₂O₃@rGO nanocomposites exhibit a faint peak at $2\theta = 12.82^\circ$, corresponding to plane (002), suggesting considerable graphite oxidation into graphene oxide (GO), and a peak at $2\theta = 42.19^\circ$, attributing to the GO's (001) plane, indicating an interlayer spacing of 0.6 nm. The grapheme sheets in rGO are stacked in an interlayer, therefore we have diffraction peaks at $2\theta = 23.85^\circ$ and $2\theta = 25.94^\circ$, which correspond to the plane (002).

FTIR analysis of Bi₂O₃@rGO nanocomposites

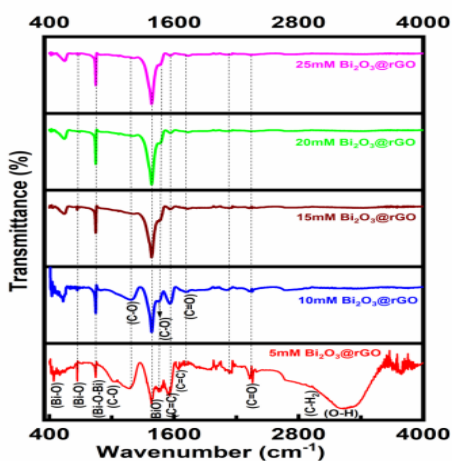


Figure 2: FTIR spectra of Bi₂O₃@rGO nanocomposite with a Bi(NO₃)₃ concentration of 5 to 25 mM

Figure 2 shows the FTIR spectrum of Bi₂O₃@rGO nanocomposites, and the spectra at 446 cm⁻¹ may be explained by the oxygen atoms being displaced around the bismuth, elongating the Bi-O bond.

Vibrational signal at 667 cm⁻¹ is due to the Bi-O bond of different lengths in deformed BiO₆ units. In the FTIR spectrum, the peak at 846 cm⁻¹ is due to the stretching vibration of the Bi-O-Bi group of the BiO₃ pyramidal unit. While a peak at 1034 cm⁻¹ was observed in the 5mM Bi₂O₃@rGO composite, corresponding to epoxy C-O stretching or alkoxy stretching, this peak is greatly attenuated in other Bi₂O₃@rGO nanocomposites as the concentration of Bi(NO₃)₃ increases. The 1177 cm⁻¹ peak is indicative of epoxy or alkoxy C-O stretching bonds.

UV-Visible measurement of Bi₂O₃@rGO nanocomposites

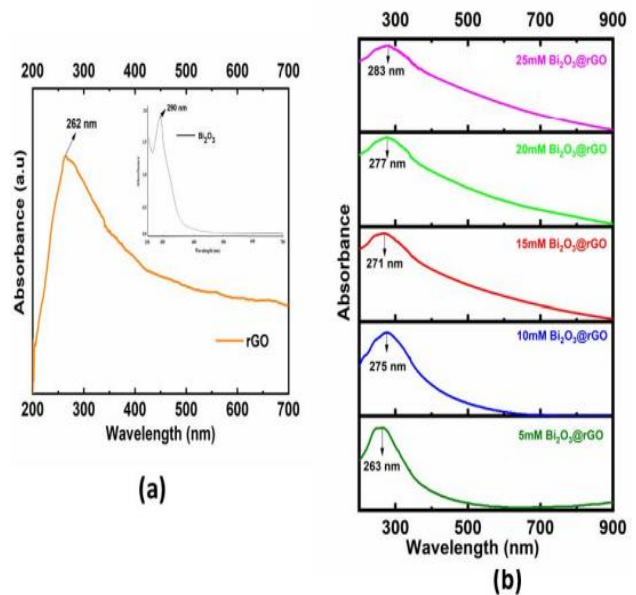


Figure 3: UV-Visible spectra of (a) pure rGO (inset bare Bi₂O₃) [212] and (b) Bi₂O₃@rGO nanocomposites with different Bi(NO₃)₃ concentrations varying from 5 to 25 mM

In Figure 3, we see the UV-Visible spectra of pure rGO, Bi₂O₃, and Bi₂O₃@rGO nanocomposites with Bi(NO₃)₃ concentrations between 5mM and 25mM. The π - π^* transitions of the C-C aromatic bond may explain the appearance at 262 nm in the UV-Vis spectra of pure rGO. the distinctive peak at 290 nm seen in the UV-Vis spectra of Bi₂O₃. Moreover, absorption peaks at 263 nm, 275 nm, 271 nm, 277 nm, and 283 nm were seen in the UV-Vis spectra of 5mM, 10mM, 15mM, 20mM, and 25mM Bi₂O₃@rGO nanocomposite, respectively, due to the presence of π transition of C-C bonds.

Absorption peak of Bi₂O₃@rGO nanocomposites is slightly shifted to the higher wavelength as the Bi₂O₃ concentration increases, as shown in UV-Vis spectra. This is because more chemical bonds are formed between the Bi₂O₃ nanoparticles and the rGO sheets, which causes the absorption peak to occur at a longer wavelength range in the rGO.

XPS analysis of Bi₂O₃@rGO nanocomposites

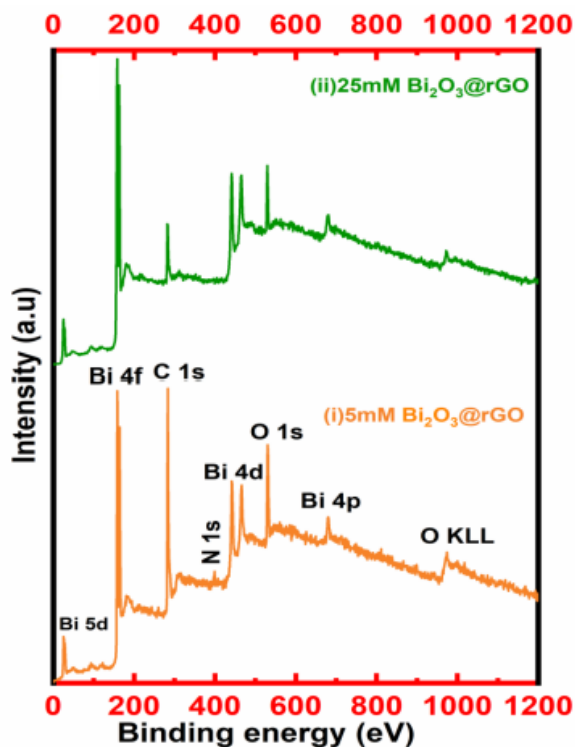


Figure 4: Scan of prepared (i) 5mM and (ii) 25mM $\text{Bi}_2\text{O}_3@\text{rGO}$ nanocomposite using XPS

The elemental chemical composition of the as-prepared $\text{Bi}_2\text{O}_3@\text{rGO}$ nanocomposite with 5mM and 25mM $\text{Bi}(\text{NO}_3)_3$ in the XPS spectra, which are depicted in Figure 4. 974.91 eV, 680.93 eV, 532.44 eV, (444.147 eV, 467.55 eV), 400.32 eV, 285.28 eV, 158.01 eV, and 25.08 eV are the values discovered for the core orbitals of the O KLL, Bi (4p), O (1s), Bi (4d), N (1s), C (1s), and Bi (5d). Here we offer an equation that can be used to calculate the atomic percentages of the obtained compositional constituents of the $\text{Bi}_2\text{O}_3@\text{rGO}$ nanocomposites.

CONCLUSION

Researchers are focusing on a scalable graphene production process that provides improved exfoliation and morphology at an inexpensive cost, for improved electrochemical performance, an electrode manufacturing technique that preserves the porosity structure and electrical characteristics of the active material, and the cell design, in order to address the two main challenges in supercapacitor research: low energy density and high cost. Several graphene-based electrode materials for supercapacitors have been produced in recent years, but researchers are still looking for innovative materials with improved specific capacitance and rate capabilities. To sum up, rGO nanocomposites based on metal/metal-oxides (M/MOs) were manufactured by a straightforward, low-cost, one-step chemical reduction approach employing hydrazine hydrate as the reducing agent. All synthesized samples were analyzed using scanning electron microscopy (SEM), X-ray diffraction (XRD), Fourier transform infrared spectroscopy (FTIR),

Raman spectroscopy (Raman), and X-ray photoelectron spectroscopy (XPS) to determine their morphology, structure, chemical bonding, vibrational signatures, defects, and elemental composition.

REFERENCES

1. Cao, G. and Wang, Y. (2nd Eds.) (2011). Nanostructures and Nanomaterials Synstudy, Properties and Applications, World Scientific Series in Nanoscience and Nanotechnology: 2, 596.
2. Fernández, J.A., Morishita, T., Toyoda, M., Inagaki, M., Stoeckli, F., Centeno, T.A. (2018). Performance of mesoporous carbons derived from poly (vinyl alcohol) in electrochemical capacitors. Journal of Power Sources, 175: 675-679.
3. Gu, D., and Schueth, F. (2014). Synstudy of non-siliceous mesoporous oxides. Chemical Society Reviews, 43: 313.
4. Karthik, M., Redondo, E., Goikolea, E., Roddatis, V., Doppiu, S., Mysyk R. (2014). Effect of mesopore ordering in otherwise similar micro/mesoporous carbons on the high-rate performance of electric double-layer capacitors. The Journal of Physical Chemistry C, 118: 27715-27720.
5. Lakra, R., Kumar, R., Sahoo, P.K., Thatoi, D., and Soam, A. (2021). A mini-review: Graphene based composites for supercapacitor application. Inorganic Chemistry Communications, 133: 108929.
6. Lee, C., Wei, X., Kysar, J.W. and Hone, J. (2008). Measurement of the elastic properties and intrinsic strength of monolayer graphene. Science, 321: 385-388.
7. Li, W., Liu, J., and Zhao, D. (2016). Mesoporous materials for energy conversion and storage devices. Nature Reviews Materials, 1: 16023.
8. Park, C.M., Kim, J. H., Kim, H. and Sohn, H. J. (2010). Li-alloy based anode materials for Li secondary batteries. Chemical Society Reviews, 39: 3115-3141.
9. Phan, T.N., Gong, M.K., Thangavel, R., Lee, Y.S., and Ko, C.H. (2018). Ordered mesoporous carbon CMK-8 cathodes for high-power and long-cycle life sodium hybrid capacitors. Journal of Alloys and Compounds, 743: 639-645.
10. Rashidi, S., Esfahani, J. A. and Hormozi, F. (2020). Classifications of Porous Materials for Energy Applications. Encyclopedia of Smart Materials, 2: 774-785.
11. Tale, B., Nemade, K.R. and Tekade, P.V. (2021). Graphene based nano-composites for efficient energy conversion and storage in Solar cells and Supercapacitors : A Review. Polymer-Plastics Technology and Materials, 60: 784-797.

12. Wu, H., Yu, G., Pan, L., Liu, N., McDowell, M.T., Bao, Z. and Cui Y. (2013). Stable Li-ion battery anodes by in-situ polymerization of conducting hydrogel to conformally coat silicon nanoparticles. *Nature Communications*, 4: 1943.
13. Yan, R., Heil, T., Presser, V., Walczak, R., Antonietti, M., and Oschatz M. (2018). Ordered mesoporous carbons with high micropore content and tunable structure prepared by combined hard and salt templating as electrode materials in electric double-layer capacitors. *Advanced Sustainable Systems*, 2: 1700128-1700139.
14. Zu, L., Zhang, W., Qu, L., Liu, L., Li, W., Yu, A., and Zhao, D. (2020). Mesoporous Materials for Electrochemical Energy Storage and Conversion. *Advanced Energy Materials*, 10: 2002152.

Corresponding Author

Shikha Upadhyay*

Research Scholar, The Glocal University